

Updates to the Regional Seismic Travel Time (RSTT) Tomography Model: Tomography and Path-dependent Uncertainty

Michael L. Begnaud¹, Stephen C. Myers², and Brian Young³

¹Los Alamos National Laboratory, ²Lawrence Livermore National Laboratory, ³Sandia National Laboratories

P1.2-120



The views expressed here do not necessarily reflect the views of the United States Government, the United States Department of Energy, the National Nuclear Security Administration, or the Los Alamos, Lawrence Livermore, and Sandia National Laboratories.

- **Abstract**
- **Introduction**
 - The Regional Seismic Travel Time (RSTT) Model
 - *Model*
 - *Prediction Uncertainty*
- **Methods**
 - Parameterization
 - Travel Times
 - Uncertainty
- **Results**
 - Tomography
 - Path-dependent Uncertainty
- **Conclusions**

ABSTRACT

A function of global monitoring of nuclear explosions is the development of Earth models for predicting seismic travel times for more accurate calculation of event locations. Most monitoring agencies rely on fast, distance-dependent one-dimensional (1D) Earth models to calculate seismic event locations quickly and in near real-time. **RSTT (Regional Seismic Travel Time)** is a seismic velocity model and computer software package that captures the major effects of three-dimensional crust and upper mantle structure on regional seismic travel times, while still allowing for fast prediction speed (milliseconds). We describe published updates to the RSTT model (**pdu202009Du**, <https://www.sandia.gov/rstt>) using a refined data set of regional phases (i.e., Pn, Pg, Sn, Lg). We improve on the former distance-dependent uncertainty parameterization for RSTT using a random effects model to estimate slowness uncertainty as a mean squared error for each model parameter. The random effects model separates the error between observed slowness and model predicted slowness into bias and random components. Validation of the updated RSTT model demonstrates significant reduction in median epicenter mislocation along with more appropriate error ellipses, compared to the *iasp91* 1D model as well as to the current station correction approach used at the Comprehensive Nuclear-Test-Ban Treaty Organization International Data Centre.

- **Most seismic monitoring agencies rely on fast travel time calculations based on distance-dependent, one-dimensional (1D) Earth models (varying with depth) in order to locate seismic events in near real-time.**
 - The complexities of the crust and upper mantle are problematic for seismic event locations when including regional seismic phases (i.e., Pn, Pg, Sn, Lg)
 - *1D models do not accurately predict regional phase travel times*
 - *Their use with regional data results in degraded event locations when combined with teleseismic phases (Bondár et al. 2004b; Myers et al. 2010).*

INTRODUCTION

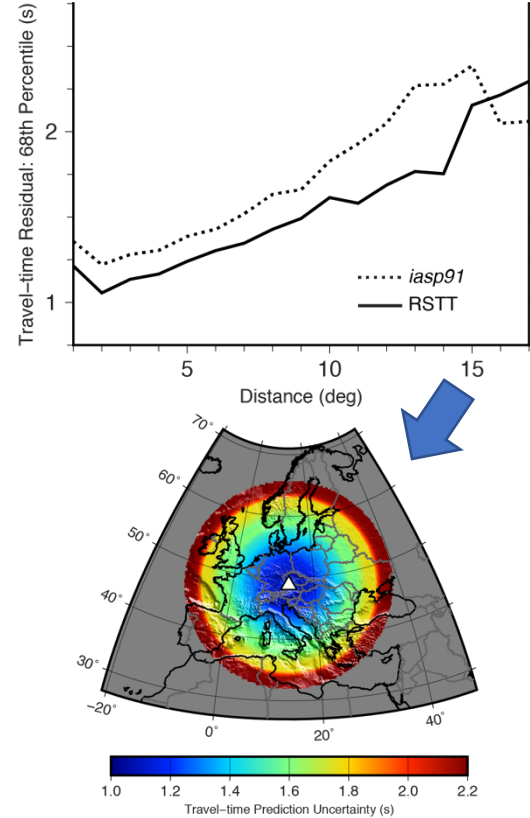
- **The RSTT (Regional Seismic Travel Time) method is a seismic velocity model and computer software package that captures the major effects of three-dimensional (3D) crust and upper mantle structure on regional seismic travel times (Myers et al. 2010).**
 - Was designed to be incorporated into real-time event location systems
 - *Travel times must be calculated in milliseconds on conventional computer hardware*
 - *Work seamlessly with travel time predictions for teleseismic P-waves that are based on standard 1D models (e.g., iasp91 (Kennett and Engdahl 1991), ak135 (Kennett et al. 1995)).*
 - *Largest improvement in location accuracy is achieved when RSTT is used with a regional network*
 - Improved accuracy is also achieved when RSTT is used with global networks like the IMS where at least a few stations are likely to be within regional distance of any given event
 - *RSTT is particularly useful for low-magnitude events where signals are more reliably detected at regional stations and those stations tend to close azimuthal gaps in network coverage*
 - Enabling regional stations to complement a teleseismic monitoring network

INTRODUCTION

• **The use of Earth models for travel-time prediction also includes estimates of prediction uncertainty or “model” error.**

- Traditionally, error estimates for higher-dimensional Earth models use a simple distance-dependent phase uncertainty estimate
 - *Treats uncertainties the same at any station, regardless of location*
- A fundamental goal of monitoring agencies is to produce location uncertainty bounds that are representative of true error,
- Higher-dimensional Earth models should include robust estimates of their prediction uncertainties in order to provide accurate size (i.e., precision) and orientations of error ellipses

Here we describe updates to the RSTT tomography model + calculation of path-dependent uncertainty, using a refined data set of Pn, Pg, Sn, and Lg phases (ONLY Pn and Pg tomography results are shown here). For **FULL results: [Tomography, Path-dependent Uncertainty](#)**



Michael L. Begnaud¹ (mbegnaud@lanl.gov), Stephen C. Myers², and Brian Young³

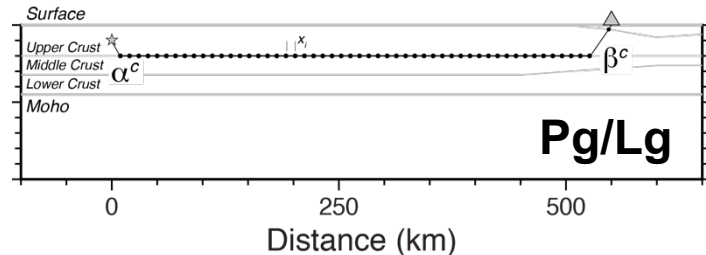
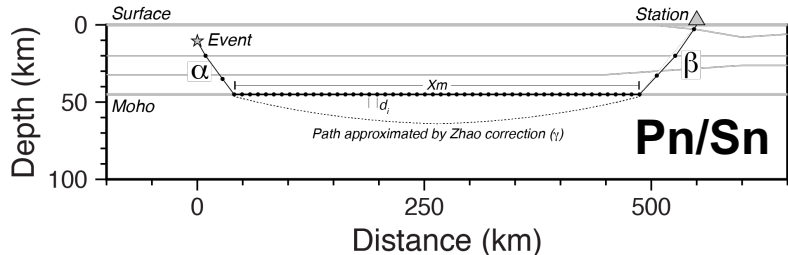
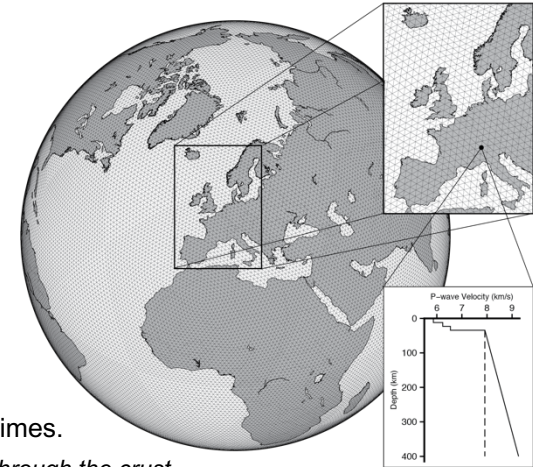
¹Los Alamos National Laboratory, ²Lawrence Livermore National Laboratory, ³Sandia National Laboratories

The Regional Seismic Travel Time Tomography Model

- The RSTT model and software are developed by the three United States National Nuclear Security Administration (NNSA) National Laboratories (Los Alamos National Laboratory, Lawrence Livermore National Laboratory, Sandia National Laboratories) in order to more accurately predict travel times from regional seismic phases ($\leq 15-18^\circ$) that typically cause degradation in event location accuracy when combined with teleseismic phases ($\geq 20^\circ$).

The RSTT model is parameterized as a global tessellation of nodes with P- and S-phase velocity profiles at each node.

- Profiles are interpolated at each node to render a 3D crust that overlies a laterally variable representation of the upper mantle velocity.
- The mantle velocity parameterization is specified by the velocity at the crust-mantle boundary and a linear velocity gradient as a function of depth.
- The model also includes an additional mid-crustal layer that is used for calculating Pg and Lg travel times.
 - This additional layer represents bulk effective wave speed for these phases which propagate horizontally through the crust.
- For a full discussion of the RSTT methodology and tomography of the Pn phase, see Myers et al. (2010).**



• Travel Time Calculation

• The full Pn/Sn travel time (TT) is defined as:

$$TT = \sum_{i=1}^N d_i s_i + \alpha + \beta + \gamma$$

- where *d* and *s* are the distance and slowness (i.e., inverse upper mantle velocity) in each of the *i* segments of the head-wave portion of the ray path, α and β are defined above, and γ is defined in Myers et al. (2010) and is related to the upper-mantle gradient.

- The method for computing travel times for Pg and Lg phases comes from Myers et al. (2007a).
- The RSTT calculation of the crustal Pg and Lg ray paths and travel times is similar to the classic definition of a P* or S* phase (Storchak et al. 2003),
 - Ray path is from the event to a mid-crustal layer, horizontally along the mid-crustal layer, then up to the station.
 - We insert a mid-crustal layer with the sole purpose of characterizing the average P-wave and S-wave velocity of horizontally propagating Pg and Lg phases, respectively.

• The full Pg/Lg travel time (T) is defined as:

$$T = \sum_{i=1}^N x_i s_i + \alpha^c + \beta^c$$

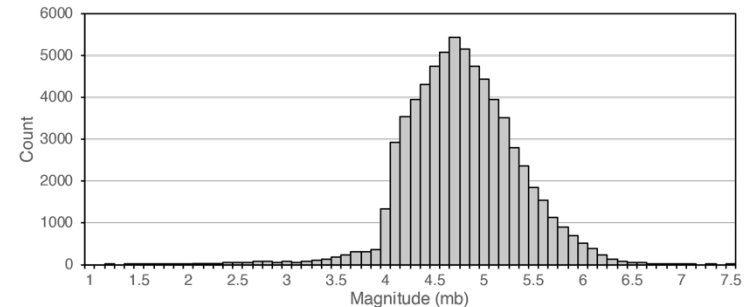
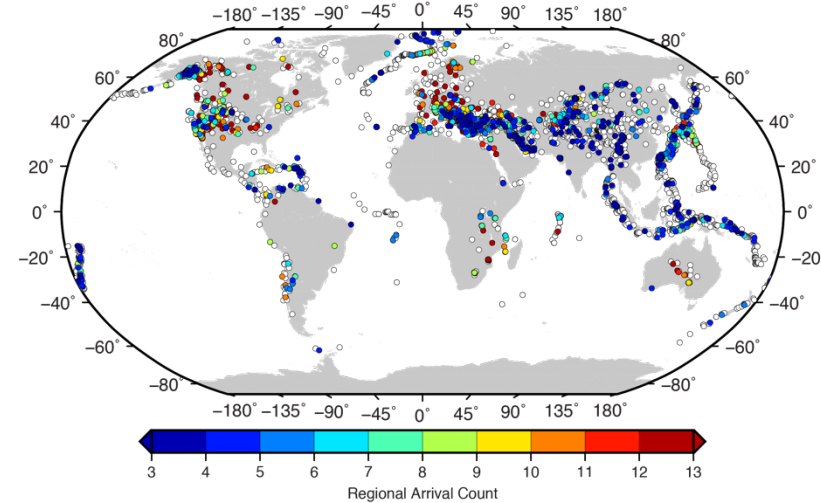
- where *x* and *s* are the distance and slowness (i.e., inverse of the mid-crustal velocity) in each of the *i* segments of the crustal head-wave portion of the ray path, and α^c and β^c are the source and receiver crustal leg portions of the travel time, respectively.

• The tomographic inversion uses the LSQR inversion algorithm (Paige and Saunders 1982), including both damping and smoothing (regularization) parameters that are optimized for the data set. The input event locations and origin times are not adjusted during tomography.

METHODS

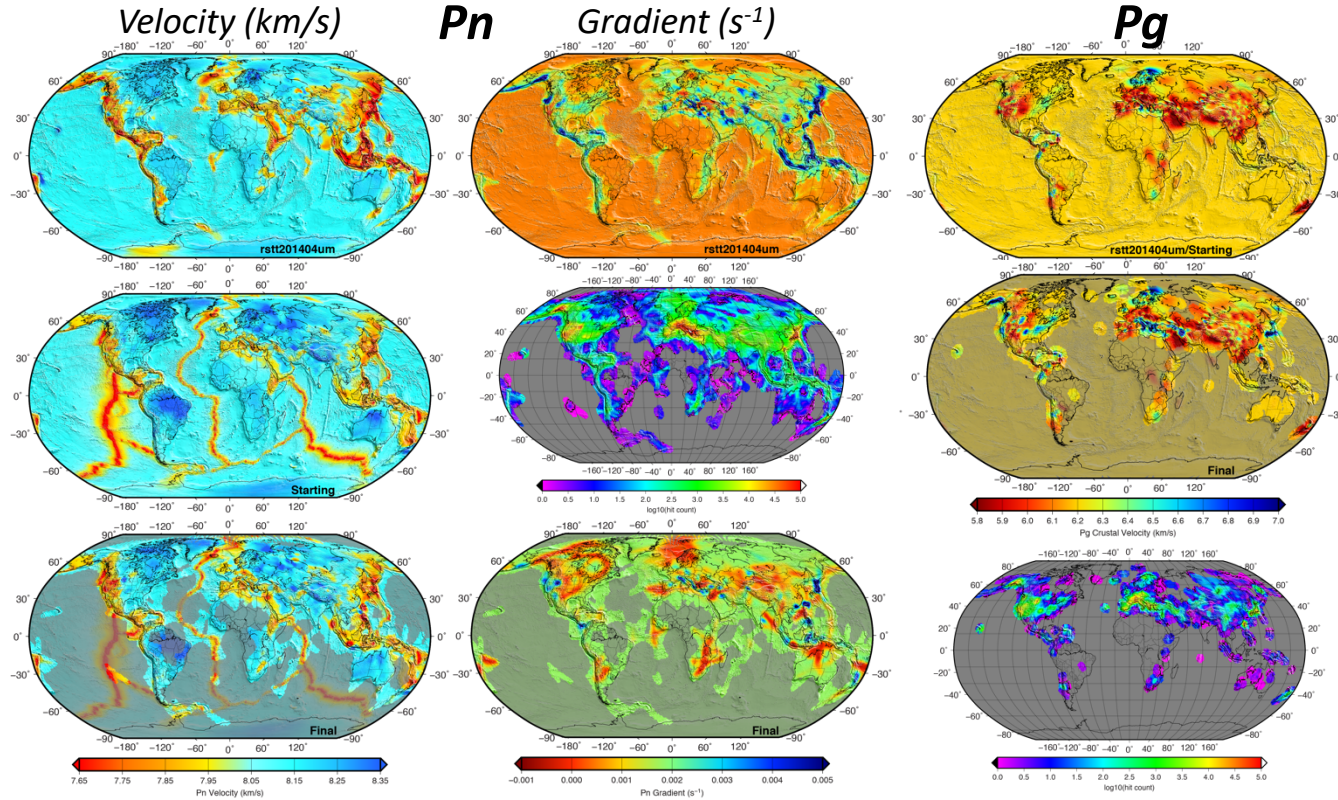
• **Tomography Data**

- (top) Subset of events (white) from the full tomographic data set in which there was a minimum of three regional phases (i.e., Pn, Pg, Sn, Lg) from the IDC Reviewed Event Bulletin (REB). This subset had preferential weighting over the remaining data during tomographic inversion. **Colored circles (indicating count of regional phases) represent validation events (30% of data set)**, randomly selected from the REB subset to leave out of the tomographic inversion and use for location testing. Validation events are sorted so events with fewer available regional phases are plotted on top. There are hundreds of events in Europe with greater than 10 available phases.
- (bottom) Distribution of reported body-wave magnitudes (68,415) for tomography data set.



Michael L. Begnaud¹ (mbegnaud@lanl.gov), Stephen C. Myers², and Brian Young³

¹Los Alamos National Laboratory, ²Lawrence Livermore National Laboratory, ³Sandia National Laboratories



Disclaimer: The views expressed on this poster are those of the author and do not necessarily reflect the view of the CTBTO PrepCom

• Path-dependent Travel-time Uncertainty

- The distance-dependent uncertainty methodology is currently a standard for seismic location. Given the 2.5D model framework for RSTT, we have the means to improve upon the standard. For a 2D model like RSTT (or 2.5D if the gradient component is considered), we want to have a path-dependent error model with a similar dimension as the model itself.

- *Evaluating the variations in residuals among model nodes will allow for a separation of the error into “model”, “bias”, and “random” components, thereby permitting a path-dependent calculation of travel-time uncertainty using a **Random Effects Model (REM)***

- We use a general error model for multiple estimates (observations) of apparent slowness (inverse velocity, [s/km]) local to a node n in the tomography model along a path i ,

- *where s_i is the apparent arrival slowness of the arrival i over its ray path, S_n is the model slowness assigned to a node n that is touched by the ray path (i.e., has a non-zero path weight), and μ_{S_n} , E_{S_n} , and ε_{S_n} are bias, model, and random error for the path slowness values at node n .*

$$s_i = (S_n + \mu_{S_n} + E_{S_n}) + \varepsilon_i$$

$$s_i - S_n = \mu_{S_n} + E_{S_n} + \varepsilon_i$$

$$S_i = \frac{(t_i - t_o) - (T_{oi,c} + T_{oi,r} + T_{oi,g})}{d_i}$$

$$S_i = \frac{T_{oi,h}}{d_i}$$

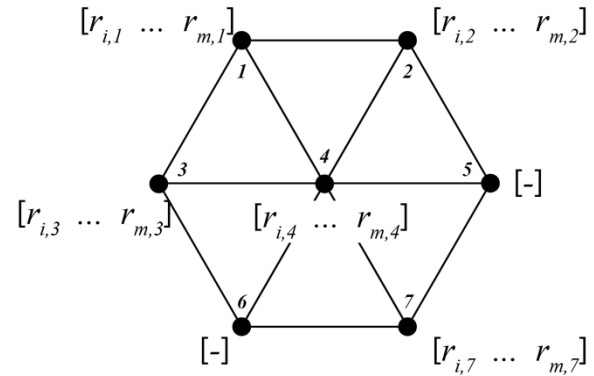
$$r_i = s_i - S_i = \frac{(t_i - t_o) - (T_{oi,c} + T_{oi,r} + T_{oi,g} + T_{oi,h})}{d_i}$$

METHODS

• Path-dependent Travel-time Uncertainty (2)

- where $(t_i - t_o)$ is the observed travel time, and $T_{oi,c}$, $T_{oi,r}$, $T_{oi,h}$, and $T_{oi,g}$ are the calculated travel times for an event o , along ray path i , for the source crustal leg c , the receiver crustal leg r , the head-wave h , and the mantle gradient portion g , and d_i is the head-wave distance (km) for path i .

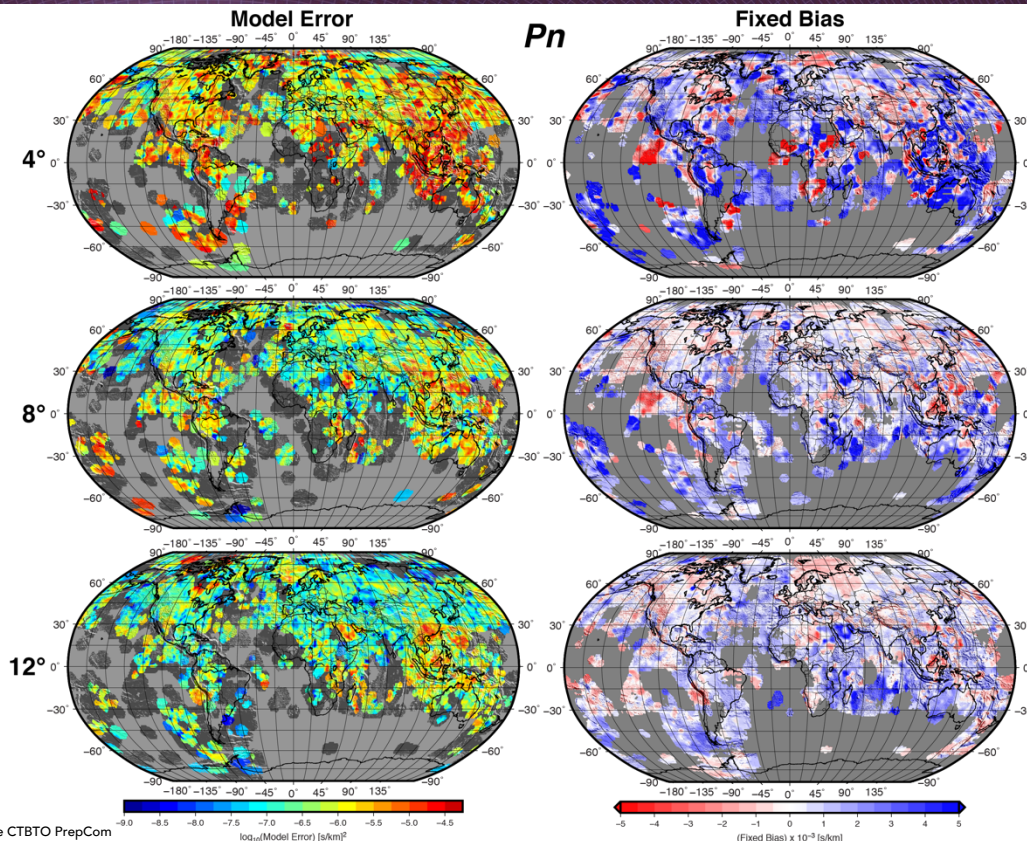
Apparent slowness residuals, r_i , are compiled for each node where rays “touch”, separated into distance bins: 2-16° @ 2° bins. The **REM** is run for each node’s residual population and saved.



Example of arrays of apparent slowness residuals ($r_{i,n}$) collected for each node n (here numbered from 1 to 7), from any subset of paths i through m . A node can have different numbers of ray paths than other nodes (each m can be different for each node), or can have no ray paths (denoted here as “-”).

RESULTS

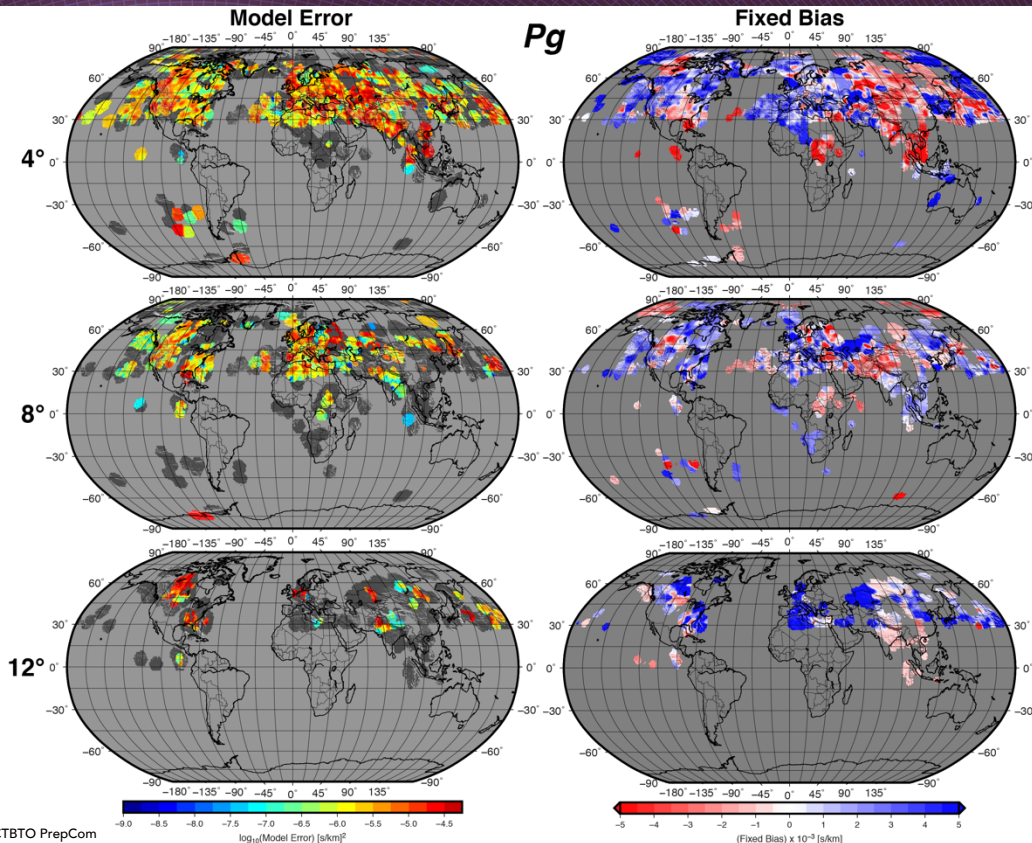
**Random
 Effects Model
 Results
 (Pn)**



Disclaimer: The views expressed on this poster are those of the author and do not necessarily reflect the view of the CTBTO PrepCom

RESULTS

**Random
 Effects Model
 Results
 (Pg)**



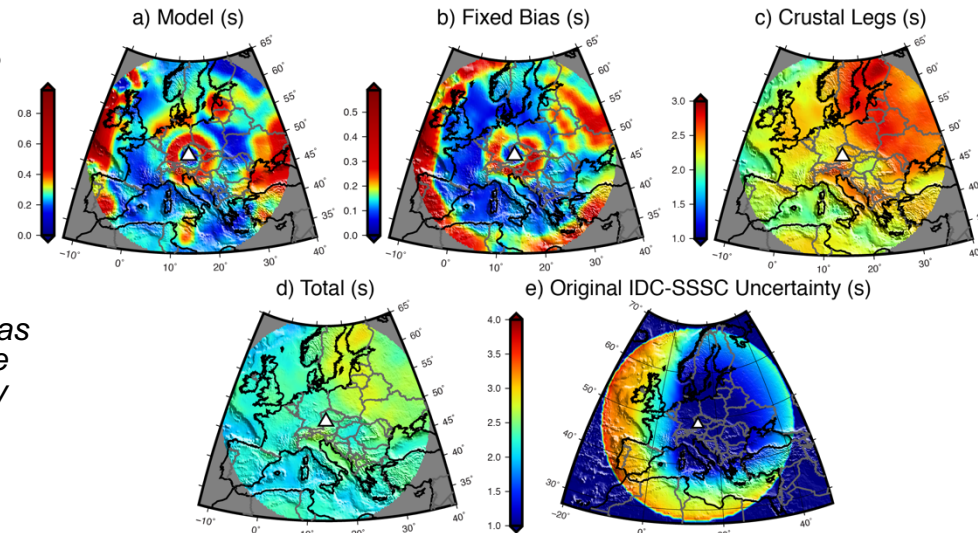
Disclaimer: The views expressed on this poster are those of the author and do not necessarily reflect the view of the CTBTO PrepCom

Calculating a Path-dependent Travel-time Uncertainty (head-wave + crustal leg)

- Head-wave:** Uncertainty (U_{hw}), path weights (w), model (τ), bias (μ), random (σ , optional)
- Crustal Leg:** Uncertainty (U_{crust}), path weights (v), percent of crustal-leg travel time (p), crustal-leg travel time ($T_{oi,c|r}$)
- Example:** Pn phase around IMS station GERES and events at zero depth.
 - (a) Model component
 - (b) Fixed Bias component
 - (c) Crustal-leg component
 - (d) Total Travel-time uncertainty
 - (e) Original IDC-SSSC total uncertainty surface (Firbas et al. 1998). Station GERES is located in a part of the tomography/validation data set where there are many ray paths for the various distance bins.

$$U_{hw} = \begin{bmatrix} w_1 & w_2 & \dots & w_n \end{bmatrix} \begin{bmatrix} \tau_1^2 + \mu_1^2 + (\sigma_{1,opt}^2) & \frac{(\tau_1^2 + \tau_2^2)}{2} & \dots & \frac{(\tau_1^2 + \tau_n^2)}{2} \\ \frac{(\tau_2^2 + \tau_1^2)}{2} & \tau_2^2 + \mu_2^2 + (\sigma_{2,opt}^2) & \dots & \frac{(\tau_2^2 + \tau_n^2)}{2} \\ \vdots & \vdots & \ddots & \vdots \\ \frac{(\tau_n^2 + \tau_1^2)}{2} & \frac{(\tau_n^2 + \tau_2^2)}{2} & \dots & \tau_n^2 + \mu_n^2 + (\sigma_{n,opt}^2) \end{bmatrix} \begin{bmatrix} w_1 \\ w_2 \\ \vdots \\ w_n \end{bmatrix}$$

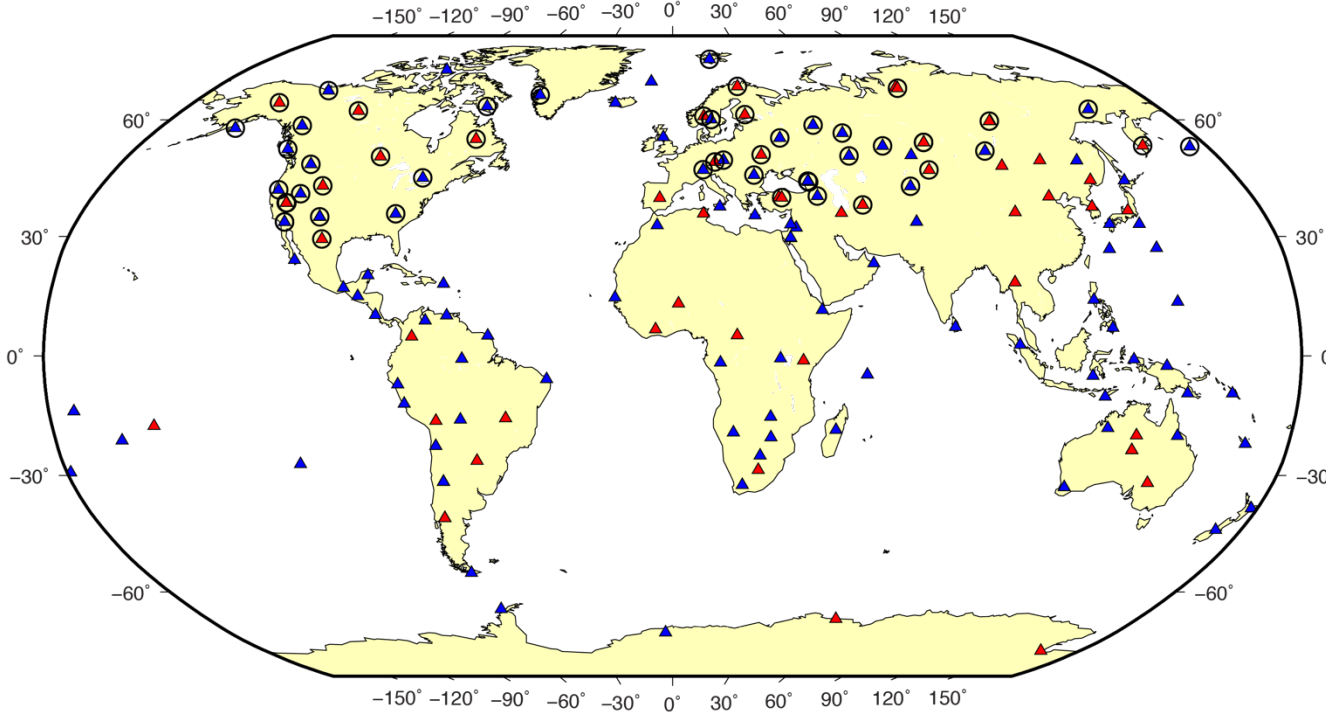
$$U_{crust} = \sum_{j=1}^m (v_j p_j T_{oi,c})^2 + \sum_{j=1}^m (v_j p_j T_{oi,r})^2$$



Michael L. Begnaud¹ (mbegnaud@lanl.gov), Stephen C. Myers², and Brian Young³

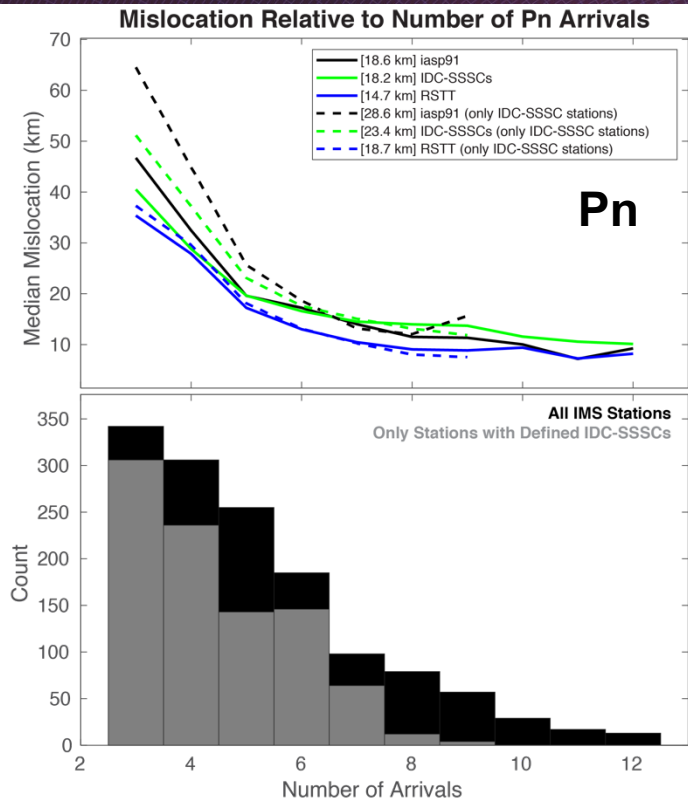
¹Los Alamos National Laboratory, ²Lawrence Livermore National Laboratory, ³Sandia National Laboratories

VALIDATION



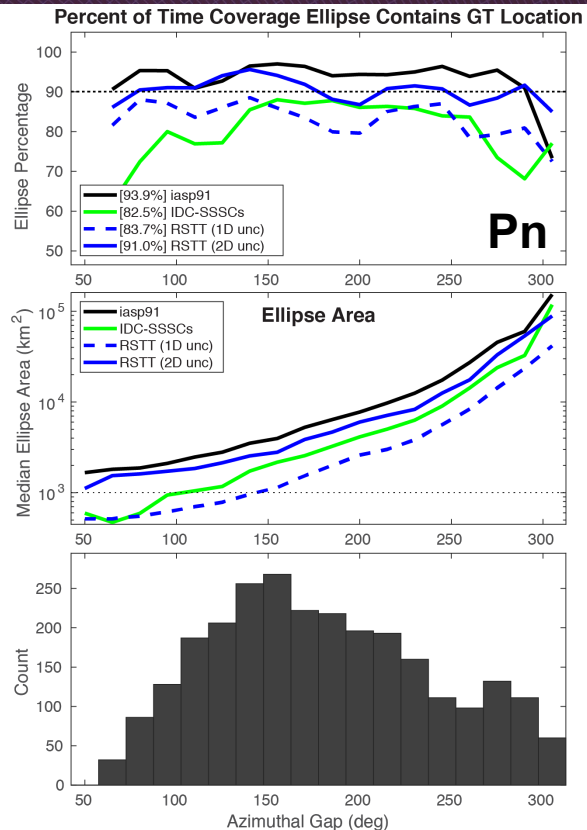
Map of International Monitoring System primary (red) and auxiliary (blue) seismic stations used for validation of model/uncertainty. Circles indicate which stations had original International Data Centre source-specific stations corrections (IDC-SSSCs) defined for regional phases (Pn, Pg, Sn, Lg) (Firbas et al. 1998).

VALIDATION

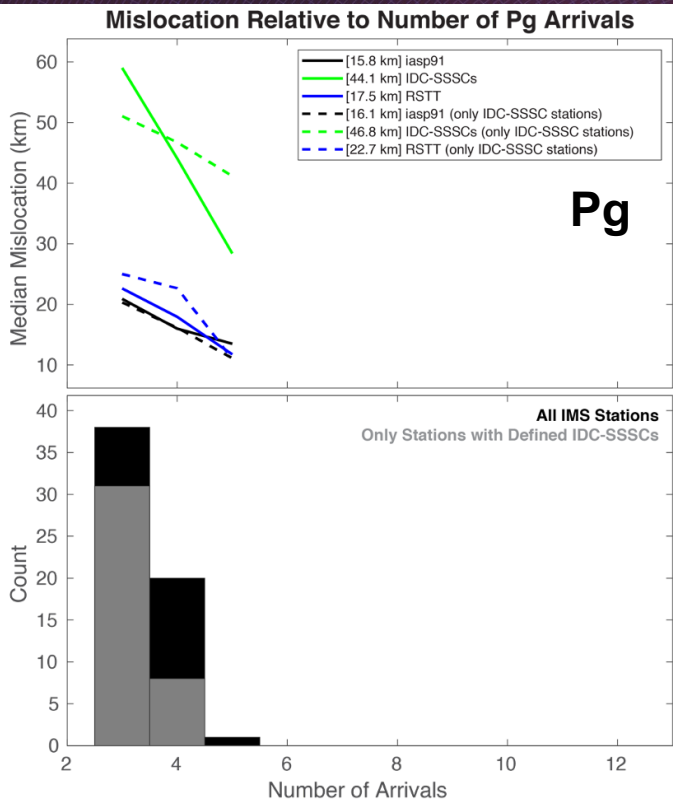


◀ Mislocation results for Pn-only relocations using the velocity models specified and all IMS stations (solid lines) or only those stations having defined IDC-SSSCs (dotted lines). (top) Median mislocation relative to the number of Pn arrivals. Overall median mislocation for each velocity model is specified in the legend. (bottom) Histogram of the number of events with specific arrival counts for the iasp91 model using all IMS stations (black) or using only those stations with defined IDC-SSSCs (gray) to demonstrate numbers of arrivals in each bin.

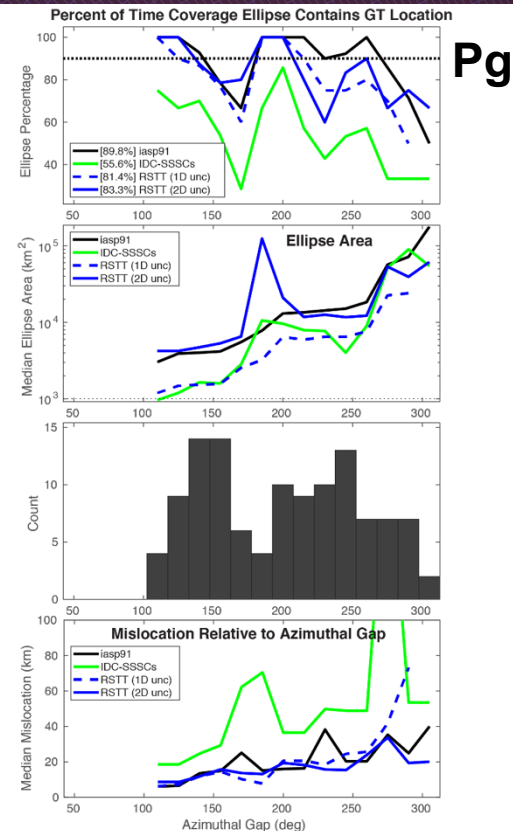
▶ Error ellipse results for Pn-only relocations using the velocity models and uncertainties specified. For RSTT, no validation events were used during tomography. (top) Percent of time the relocation 90% coverage ellipse contains the GT location. The 90% coverage ellipse line is shown. Azimuthal gap bins are every 15° and overlap by 1. (bottom) Histogram of counts per azimuthal gap for the iasp91 model to demonstrate numbers of arrivals in each bin



VALIDATION

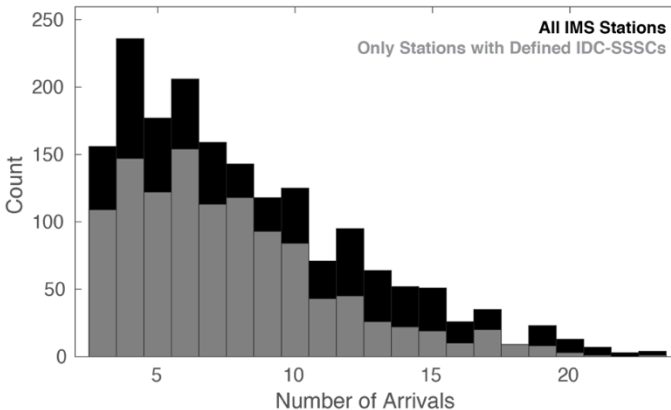
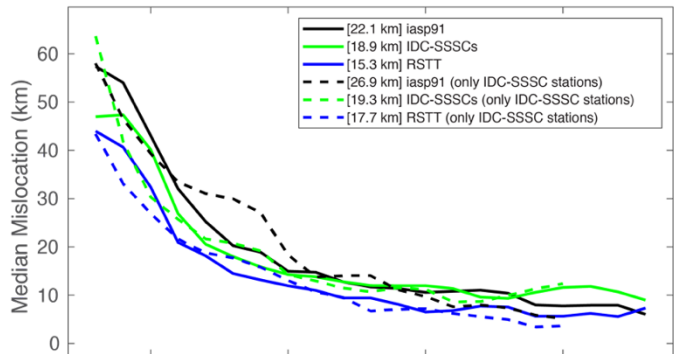


Mislocation (LEFT) and Error ellipse (RIGHT) validation results for Pg-only relocations. See Pn validation slide for plot characteristics.



VALIDATION

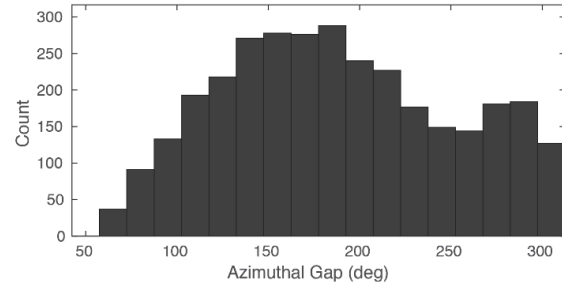
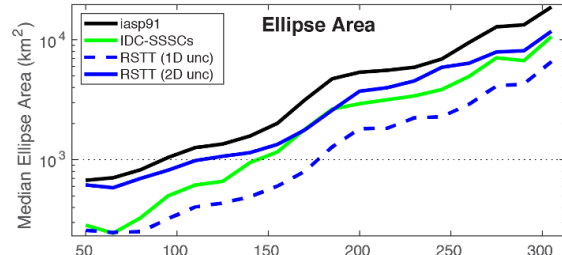
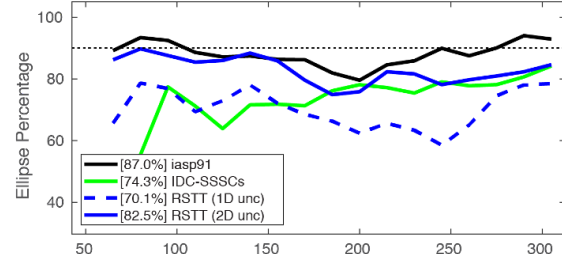
Mislocation Relative to Number of Arrivals



All Regional

Mislocation (LEFT) and Error ellipse (RIGHT) validation results for All-regional Phase (Pn, Pg, Sn, Lg) relocations. See Pn validation slide for plot characteristics.

Percent of Time Coverage Ellipse Contains GT Location



CONCLUSIONS

- **The RSTT model has been updated to version *pdu202009Du* and is publicly available (<https://www.sandia.gov/rstt>)**
 - New data set based on Bayesloc
 - Now includes path-dependent travel-time uncertainty
- **Tomography**
 - Includes all four regional phases (Pn, Pg, Sn, Lg)
 - Results in a significant reduction in median mislocation values over other tested models
- **Path-dependent Travel-time Uncertainty (PDU)**
 - Used a ***Random Effects Model*** to develop error values (model, bias, random) that can be combined with individual nodal path weights to calculate a travel-time uncertainty
 - Validation results indicate that using the PDU results in 90% coverage ellipse sizes that more closely reach the target error ellipse percentage (ground-truth event within the relocated error ellipse, 90% of the time)

- Bondár, I., Myers, S. C., Engdahl, E. R., & Bergman, E. A. (2004b). Epicentre accuracy based on seismic network criteria. *Geophysical Journal International*, 156, 483-496.
- Firbas, P., Fuchs, K., & Mooney, W. D. (1998). Calibration of seismograph network may meet Test Ban Treaty's monitoring needs. *EOS, Transactions of the American Geophysical Union*, 79, 413-421.
- Kennett, B. L. N., & Engdahl, E. R. (1991). Traveltimes for global earthquake location and phase identification. *Geophysical Journal International*, 105(2), 429-465.
- Kennett, B. L. N., Engdahl, E. R., & Buland, R. (1995). Constraints on seismic velocities in the Earth from travel times. *Geophysical Journal International*, 122, 108-124.
- Myers, S. C., Begnaud, M. L., Ballard, S., Pasyanos, M. E., Phillips, W. S., Ramirez, A. L., et al. (2010). A crust and upper mantle model of Eurasia and North Africa for Pn travel time calculation. *Bulletin of the Seismological Society of America*, 100(2), 640-656.
- Storchak, D. A., Schweitzer, J., & Bormann, P. (2003). The IASPEI standard seismic phase list. *Seismological Research Letters*, 74(6), 761-772.
- Paige, C. C., & Saunders, M. A. (1982). LSQR: An algorithm for sparse linear equations and sparse least squares. *ACM Trans. Math. Softw.*, 8(1), 43-71.